CONF-850398--2

EXTENDED OVERPOWER TRANSIENT TESTING OF LMFBR OXIDE PINS IN EBR-II

by

Hanchung Tsai and L. A. Neimark
Argonne National Laboratory, USA

and

S. Tani and I. Shibahara
Power Reactor and Nuclear Fuel Development Corporation
Japan

CONF-850398--2

DE85 006126

Abstract

As part of a joint effort between the Power Reactor and Nuclear Fuel Development Corp. of Japan and the U.S. Department of Energy, a series of five extended slow overpower transient tests are being conducted in the Experimental Breeder Reactor-II (EBR-II) on preirradiated mixed oxide fuel and blanket pins. In the first two tests conducted in the series, fuel and blanket pins were subjected to a 0.1%/s power ramp to ~60% overpower before the transient termination. None of the test pins breached during the transient. A significant cladding breaching margin over the normal PPS trip setting of ~12-15% was thus demonstrated for the 0.1%/s ramp. The transient-induced pin cladding strains, caused principally by fuel-cladding mechanical interaction, were small but measurable.

I. INTRODUCTION

Understanding the behavior of oxide fuel and blanket pins during slow overpower transients, i.e., <10% $\Delta P/P_0/s$, is important because of the higher likelihood of such operational transient events compared with the fast transients normally associated with hypothetical core disassembly events. A large body of data exists for the fast transient, principally from the in-pile testing conducted in the Transient Reactor Test facility (TREAT); few data exist on the possible vulnerability of oxide pins to slow transients, however. Such vulnerability of oxide pins to slow transients was postulated in an earlier analysis (ref. 1) and was thought to be partly the cause of the cladding breaching in a test pin in the TREAT HOP-1-6A test which simulated a ~3%/s transient to 25% overpower (ref. 2).

A cooperative program between the U.S. Department of Energy and the Power Reactor and Nuclear Fuel Development Corp. (PNC) of Japan is being conducted in the Experimental Breeder Reactor-II (EBR-II) to investigate various effects of slow transients and duty cycles on oxide pin behavior. The extended overpower transient test series, which is the subject of this paper, is part of this program. One of the principal objectives of the extended overpower transient tests is to address the vulnerability issue by investigating the breaching margins of oxide fuel and blanket pins above the plant protection system trip settings, nominally 12 and 15%, over a range of ramp rates. The performance data obtained from these tests will be used to validate the fuel and blanket behavior codes, such as LIFE-4 (ref. 3) and CEDAR (ref. 4), and to enhance their predictive capabilities. As transient tests in EBR-II can be initiated from true steady-state conditions, while those in TREAT are limited to preconditioning of much shorter durations (typically seconds), one of the tests in this series will be designed as a comparative test (with a ramp rate that can be achieved in both facilities) to evaluate the effects of preconditioning. This will provide a significant linkage between the EBR-II and the TREAT data bases.

II. TEST DESCRIPTION

Transient overpower of test pins in EBR-II, a normally steady-state reactor, is achieved by first relocating pins that were preirradiated in the lower power, outer row positions into the center of a specially configured core designed for power peaking. In this new location the test pins are

preconditioned at a partial reactor power that produces the nominal steady-state heat rating in the relocated test pins. The preconditioning period is either two or seven days, depending on the power level, to re-establish the prior steady-state thermal and mechanical balance in the test pins. The reactor power is then slowly increased at the prescribed ramp rate to the administrative power limit. To maximize the achievable overpower, only pins that were irradiated in the outermost rows (5 and 6) in EBR-II were selected for this series of tests. At the present EBR-II power limit of 62.5 MWt, the maximum overpower achievable in available test pins is approximately 95%. For the later tests in the series, the EBR-II power limit for transients may be raised to 75 MWt, which would provide a peak overpower of ~135% in the test pins.

Of the five tests in the series, four (designated TOPI-1A, 1B, 1C, and 1D) were on preirradiated mixed oxide fuel pins, and the other (TOPBI-1) was on preirradiated oxide blanket pins. A summary description of these tests is given in Table 1. The tests cover a range of ramp rates (0.1 to 10%/s) and overpower (60% to 135%) and include test pins with various design variables. Each of the tests employs a dedicated subassembly consisting of 19 fuel pins or 7 blanket pins. Tests TOPI-1A and TOPBI-1 were conducted in February 1983 and are the subject of this paper; the other three tests are either just completed or still in the planning stage.

Sixteen of the 19 fuel pins for the TOPI-1A test were obtained from a steady-state experiment, designated P43 (ref. 5), in EBR-II. The other three pins were fresh fuel pins of similar designs. The principal design and operating variables of the test pins in the TOPI-1A test were fuel smear density, plenum size and location, cladding type, and fuel burnup, as shown in Table 2. A number of aggressively designed P43-B-, P43-C-, and P43-F-type pins with high fuel smear density were included in the TOPI-1A test for the purpose of accentuating the transient-induced effects. Also shown in Table 2 are the peak overpower achieved in each of the test pins during the TOPI-1A test. While the subassembly average overpower was 62%, because of the different end-of-life conditions of the test pins, the range of peak overpower was 54 to 68%.

The blanket pins for the TOPBI-1 test consisted of four pins from a steady-state experiment (designated W21) and three additional W21 pins from ar

EBR-II test (designated W24) whose irradiation consisted of 54 power cycles between 46 and 121% nominal pin power and a final transient to 151% power. The W21 pins were originally designed to investigate the performance of large-diameter (12.85-mm) blanket pins at peak power and temperature conditions. The key design parameters, prior irradiation histories, and achieved peak overpower of the blanket pins in the TOPBI-1 test are shown in Table 3.

The EBR-II reactor power history during the TOPI-1A test is shown in Fig. 1; that for the TOPBI-1 tests was quite similar. These two transients were achieved by manual withdrawal of a control rod at a predetermined speed and then scramming at the peak power. An automatic control rod drive system has since been installed at EBR-II that will provide a greater range of achievable ramp rates for the later tests in the series.

III. TEST RESULTS

The significant nondestructive examination results of the TOPI-1A and TOPBI-1 tests are presented below; no data on the destructive examination of the test pins are available at this time.

A. Cladding integrity limits

During the TOPI-1A and TOPBI-1 transients, the EBR-II open-core delayed-neutron detection system and the cover-gas monitoring system were monitored closely to detect any pin cladding breaching during the tests. Neither system showed activity profiles above the background, thus indicating no pins had breached because of the applied transients. Leak checking of the sub-assemblies after their discharge from the reactor provided the positive confirmation. A cladding integrity margin of at least 60% overpower was thus demonstrated for the test fuel and blanket pins for the 0.1%/s ramp.

Compared to the normal trip settings for a plant protection system of 12-15% overpower, the demonstrated margin of >60% is substantial in supporting the LMFBR plant operation and the licensability of mixed oxide fuel and blanket systems against single, slow overpower transient events.

B. Thermal Effects

Thermal effects, such as fuel melting, fuel microstructural changes, or release of fission products, may be used to aid the calibration of fuel behavior codes and are being evaluated for the TOPI-1A and TOPBI-1 test pins.

Among the TOPI-1A test pins, the fresh P40 pins had the highest linear power (51 kW/m at the transient peak), and incipient centerline fuel melting in these pins was predicted. The posttest neutron radiographs showed formation of intermittent central voids of various size along the midsection of the pins, suggesting that fuel melting and some slumping occurred in these three pins. The radiograph of one such fresh pin, P40-C44, is shown in Fig. 2. For the preirradiated P43 pins, which had linear powers 5-10 kW/m lower than the P40 pins at the peak of the transient, no clear indications of transient-induced fuel melting could be noted.

The neutron radiographs revealed significant axial movement, both upward and downward, of solid fission products in the central void of some P43 pins. An example is shown in Fig. 3, which compares the pretest and posttest radiographs of a 6.1 a/o burnup pin, P43-C29. Individual ingots present in the upper portion of the P43-C29 pin before the transient collected to form an almost continuous ingot in the upper 35 mm of the central void. It is postulated that this compaction resulted from the expansion of hot gas during the transient in the probably sealed-off central void. Inward radial movement of solid fission products also occurred during the transient, particularly in the higher burnup pins. New ingots in the central void were found in these pins.

The neutron radiographs of the TOPBI-1 pins indicated that, with peak pin power exceeding 60 kW/m, centerline fuel melting occurred in all seven pins during the TOPBI-1 transient. The comparison of pretest and posttest radiographs of pin W21-9 is illustrated in Fig. 4. Fuel melting and downward slumping of molten fuel apparently filled the central void in the lower half of the fuel column while creating a large freeze cavity above the midplane. Significantly, the extensive fuel melting and motion in these high smear density (93% TD) blanket pins did not cause any of the pins to breach. Also associated with fuel melting is the precipitation of metallic fission-product ingots in the higher burnup, steady-state irradiated W21 pins; the axial location where the ingots were found corresponds closely to the lower extent of the steady-state central voids of these pins.

C. Cladding strain

Prior to the transient testing, the cladding diameter profiles of the test pins were measured with a laser profilometer at the Hot Fuel Examination Facility (HFEF). Three pins, P43-A5 and -A8 of the TOPI-1A test and W21-08 of

the TOPBI-1 test, had no spacer wires and were scanned linearly at 9° azimuthal intervals. For these three pins, the cladding diameter was obtained by averaging all the azimuthal measurements. The other pins in the TOPI-1A and TOPBI-1 tests had the spacer wires attached and were scanned spirally along pre-mapped paths (approximately 90° from the wire) that avoided interference between the wires and the profilometer. The spiral measurements were performed twice over at paths at 0° and 180° to check the diameter reproducibility. Following the transient testing, identical linear and spiral profilometry measurements were performed to determine the transient-induced increments of cladding strain.

The measured incremental strain profiles of the test fuel pins are illustrated in Figs. 5 and 6 for fuel pins P43-F104 and P43-A5, respectively. The incremental strain profile for pin P43-F104, with 90% fuel smear density and 0.38-mm-thick D9 cladding, showed little strain in the lower half of the fuel column but increasing strain with elevation in the upper half. This observation is in good agreement with the LIFE-4 and CEDAR code calculations which predicted the incremental strain would peak near the top because of the lower creep resistance of the cladding at the hot end. The codes also predicted fuel-cladding mechanical interaction (FCMI), caused mostly by differential thermal expansion, to be the dominant loading mechanisms on the cladding. The fact that the observed cladding incremental strain profile shows a marked decrease in the plenum region above the fuel stack supports the conclusion that FCMI, rather than fission-gas loading, was the primary loading mechanism in this high smear density, D9-clad pin. A similar conclusion can be drawn for the other high smear density fuel pins in the test.

In the P43-A5 pin, which had an 85% smear density and a 0.38-mm-thick 316 SS cladding, FCMI was less pronounced and the transient-induced cladding strain, shown in Fig. 6, was quite small, less than 0.04% max. The strain profile again shows a trend of increasing strain with increasing elevation, or cladding temperature. A small increase in cladding diameter appears to have developed in the plenum region above the 12.7-mm-high UO_2 insulator pellet, which suggests that part of the cladding strain observed in the fuel column region was caused by fission-gas loading in this pin.

The 60% overpower transient also resulted in incremental cladding strains in the blanket pins of the TOPBI-1 test. The incremental cladding strain profile for pin W21-08, a typical pin, is shown in Fig. 7. A nearly uniform incremental strain on the order of approximately 0.1% occurred in the top one-third of the fuel column. The local strain peaks found in this region coincide consistently with pellet-pellet interfaces, indicating the observed deformation was due to fuel cladding mechaical interaction and, specifically, fuel pellet hour-glassing. In the midplane region where extensive fuel melting and slumping occurred (Fig. 4), the pronounced irregular strain pattern appears to be the result of loading due to the fuel volumetric expansion upon melting. This was probably accentuated by the fact that the blanket test pins had a relatively high smear density of 93% and therefore little porosity within the fuel to accommodate the volumetric expansion. There was no measurable cladding deformation in the plenum region above the top insulator, indicating that fission-gas pressure in this low-burnup blanket pin was insignificant.

IV. DISCUSSION

The TOPI-1A and TOPBI-1 tests, performed under prototypic fast reactor conditions, showed that even aggressively designed mixed-oxide fuel and blanket pins can withstand a slow overpower transient to 60% overpower with no cladding breaching. The breaching margins for reference design fuel and blanket pins, with lower smear densities, would likely be even greater. These are substantial margins in light of the extended duration of the event, on the order of minutes, during which time ample corrective actions may be taken by the plant operators to terminate the reactivity insertion. The earlier concerns that mixed-oxide pins may be particularly vulnerable to slow transients have not been substantiated for the conditions of the tests described or the combination of design and operation variables tested.

The cladding incremental strain data from the entire population of the TOPI-1A and TOPBI-1 tests revealed a dependency of strain on fuel smear density and cladding fluence. Among pins with similar burnup, greater incremental strains were found in pins with greater fuel smear densities. Among pins with the same smear densities and the same Type 316 stainless steel cladding, incremental strains appear to peak in pins with low to intermediate fast fluence ($\sim 4 \times 10^{22}$ n/cm^2), i.e., before cladding swelling accelerated. This suggests that the reduced strains in the higher fluence and burnup pins

benefitted from cladding swelling, which alleviated FCMI. Similarly, the comparison of strains in 316-clad and D9-clad pins with about the same burnup and fluence revealed greater incremental strains in the more swelling-resistant D9-clad pins. The plenum-to-fuel volume ratio in the test pins ranged from 1.3 to 1.6, and the calculated plenum pressure at the peak of the transient ranged from 1.5 to 9.3 MPa. Within the accuracy of the data, there appears to be no clear relationship between the overall strain and the plenum pressure, suggesting fission gas loading was in general insignificant during the transient.

It is generally agreed that fuel pin behavior up to the point of cladding breaching is dominated by thermally induced volume expansion of fuel relative to the cladding. The causes of fuel volume expansion include thermal expansion, swelling due to fission-gas bubble growth or fuel microcracking, and, probably most important, fuel melting. The results from the TOPI-1A and TOPBI-1 tests appear to be in substantial agreement with this assessment. As all forms of voids inside the cladding (such as the central void, startup and shutdown cracks, and the fuel-cladding gap) that can accommodate fuel volume expansion can potentially impact the integral pin behavior, the ability to heal the shutdown cracks (particularly those in the circumferential direction) and close the fuel cladding gap with sufficient preconditioning in EBR-II makes such tests particularly meaningful.

V. CONCLUSIONS

The following conclusions were derived from the available results of the TOPI-1A and TOPBI-1 tests:

1. Mixed-oxide fuel and blanket pins are capable of withstanding a 0.1%/s overpower transient with a severity significantly greater than the normal PPS trip setting without cladding breaching,
2. Even though no data on cladding breaching mode and mechanism were generated, the other results from the tests, such as cladding strain and fuel thermal performance, offer valuable data to enhance the understanding of the transient behavior of mixed oxide pins during a slow overpower transient,
3. To achieve cladding breaching for the purpose of establishing breaching criteria, higher overpower (>60%) and more aggressive test pin designs would be required.

VI. ACKNOWLEDGMENTS

We wish to acknowledge the support from DOE and PNC for this test program. Guidance from Dr. A. Boltax of Westinghouse-Advanced Energy System Division, the technical manager of this program, is deeply appreciated. The operational support provided by the competent people at EBR-II and HFEF is also gratefully acknowledged. Special appreciation is extended to HEDL and Westinghouse-AESD for the supply of the test fuel pins.

VII. REFERENCES

1. Boltax, A. and Sackett, J. I. A proposed program for operational transient testing of breeder reactor fuel. Proceedings of ANL Topical Meeting on Reactor Safety Aspects of Fuel Behavior, 1981, August.

2. Duncan, D. R. et al. Comparison of in-reactor and out-of-reactor fuel pin cladding strain under transient loading. Transactions of the American Nuclear Society, 1979, vol. 32, 221-223.

3. Roth, T. S. et al. Modeling of fast reactor fuel transient behavior using the LIFE code. Proceedings of the International Conference on Fast Breeder Reactor Performance, 1979, March.

4. Nagai, H. et al. A development of fast breeder reactor fuel pin performance code - CEDAR. Presented at the 1983 Annual Meeting of the Atomic Energy Society of Japan, 1983, March.

5. Cox, C. M. and Hilbert, R. F. U.S. experience in irradiation testing of advanced oxide fuels. Proceedings of the ANS Topical Meeting on Advanced LMFBR Fuels, 1977, October.

Table 1. Key Test Parameters

	TOPI-1A	TOPI-1B	TOPI-1C	TOPI-1D	TOPBI-1
Pin Type	Fuel	Fuel	Fuel	Fuel	Blanket
Pin Dia., mm	5.8	5.8	5.8	5.8, 7.0	12.9
No. of Pins	19	19	19	19	7
Pin Source	P43, 40	P43, 40, 14A	P43, 40, 14A	TOP4, 7	W-21, 24
Prior History	SS	SS, +TOP	SS	SS	SS, +TOP
SS EBR-II Row	6	6	6	5, 2	5
Cladding Type	316, D9	316, D9	316	316, D9	316
SS LWR, kW/m	22-32	15-31	15-30	30-40	38-41
Tr. Clad T., C	760	780	800	800	760
Ramp, %/s	0.1	10.0	0.1	0.1	0.1
Overpower, %	62	95	110	110	60

Table 2. Key Design and Irradiation Parameters for TOPI-1A Test Pins

	Design				Pretransient				Transient	
Pin[1]	Pellet Density (%TD)	Dia. Gap (mm)	Smear Density (%TD)	O/M	BOL Peak Clad. Temp (°C)	EOL Peak Pin Power (kW/m)	Peak Burnup (a/o)	Peak Fast Fluence ($\times 10^{22}$ n/cm^2)	Peak Precond. Power (kW/m)	Peak Transient[2] Overpower (%)
P43-A5	89.3	0.11	85.4	1.936	645	26	6.1	4.2	26	57
P3-A6	89.3	D.11	85.4	1.936	635	27	6.2	4.3	26	54
P43-A8	89.3	0.11	85.4	1.936	620	22	16.4	12.1	22	62
P43-A9	89.3	0.11	85.4	1.936	645	26	6.1	4.2	26	57
P43-A10	89.3	0.11	85.4	1.936	640	26	4.1	2.7	27	63
P43-A11	89.3	0.11	85.4	1.936	640	26	4.1	2.7	27	64
P43-B16	95.4	0.13	90.7	1.936	640	26	5.8	4.0	28	68
P43-B18	95.4	0.13	90.7	1.936	650	26	5.8	4.0	28	58
P43-C29	93.4	0.08	90.6	1.936	645	27	6.1	4.2	27	59
P43-C32	93.4	0.08	90.6	1.936	600	28	6.1	4.2	27	57
P43-C33	93.4	0.08	90.6	1.936	640	24	12.3	8.9	25	62
P43-C34	93.4	0.08	90.6	1.936	650	25	12.1	8.8	25	62
P43-C35	93.4	0.08	90.6	1.936	650	25	12.0	8.6	25	62
P43-C40	93.4	0.08	90.6	1.936	605	24	11.8	8.5	25	65
P43-F103	96.2	0.17	89.8	1.955	650	25	10.5	7.4	25	67
P43-F104	96.2	0.17	89.8	1.955	650	25	10.5	7.4	25	67
P40-C41	93.2	0.12	88.8	1.951	---	---	0	0	32	59[2]
P40-C44	93.2	0.12	88.8	1.951	---	---	0	0	32	59[2]
P40-C45	93.2	0.12	88.8	1.951	---	---	0	0	32	59[2]

(1) All pins have 5.84 mm OD, 0.38 mm thick, Type 316 SS 20% CW cladding, except for P43-F103 and F104 which have 20% CW D9 cladding of the same dimensions. The fuel column length and pin length are 343 and 1540 mm, respectively.

(2) For the preirradiated pins, peak overpower are with respect to the EOL peak pin power. For the fresh P40 pins, overpower are with respect to the linear power during preconditioning period.

Table 3. Key design and irradiation parameters for TOPBI-1 test pins

	Design				Pretransient					Transient	
Pin[a]	Pellet density: %TD	Dia. gap: mm	Smear density: %TD	O/M	History	BOL peak clad. temp.: °C	EOL peak pin power: kW/m	Peak burnup: a/o	Peak Fast fluence: $\times 10^{22}$ n/cm^2	Peak precond. power: kW/m	Peak transient[b] overpower: %
W21-1	95.9	0.09	94.5	2.002	W21	500	39	2.6	9.2	40	65
W21-6	95.9	0.09	94.5	2.002	W24	---	---	0.1	0.3	42	61[c]
W21-8	95.9	0.09	94.5	2.002	W21	645	40	2.9	10.3	40	58
W21-9	95.9	0.08	94.5	2.002	W21	645	41	2.9	9.9	40	57
W21-13	94.7	0.16	92.1	2.002	W21	645	41	2.9	10.5	39	52
W21-17	94.7	0.16	92.1	2.002	W21 & W24	640	38	2.8	9.6	39	65
W21-19	94.7	0.16	92.1	2.002	W21	---	---	0.1	0.3	41	61

(a) All pins have 12.85 mm OD, 0.38 mm thick, 20% CW Type 316 SS cladding. The fuel column length is 343 mm.

(b) W21 was a steady-state irradiation. W24 was a run consisting of cyclic transients (see text).

(c) W21-6 and -19, irradiated in W24, had no well-defined steady-state preirradiation; overpower during transient is based on linear power during preconditioning period.

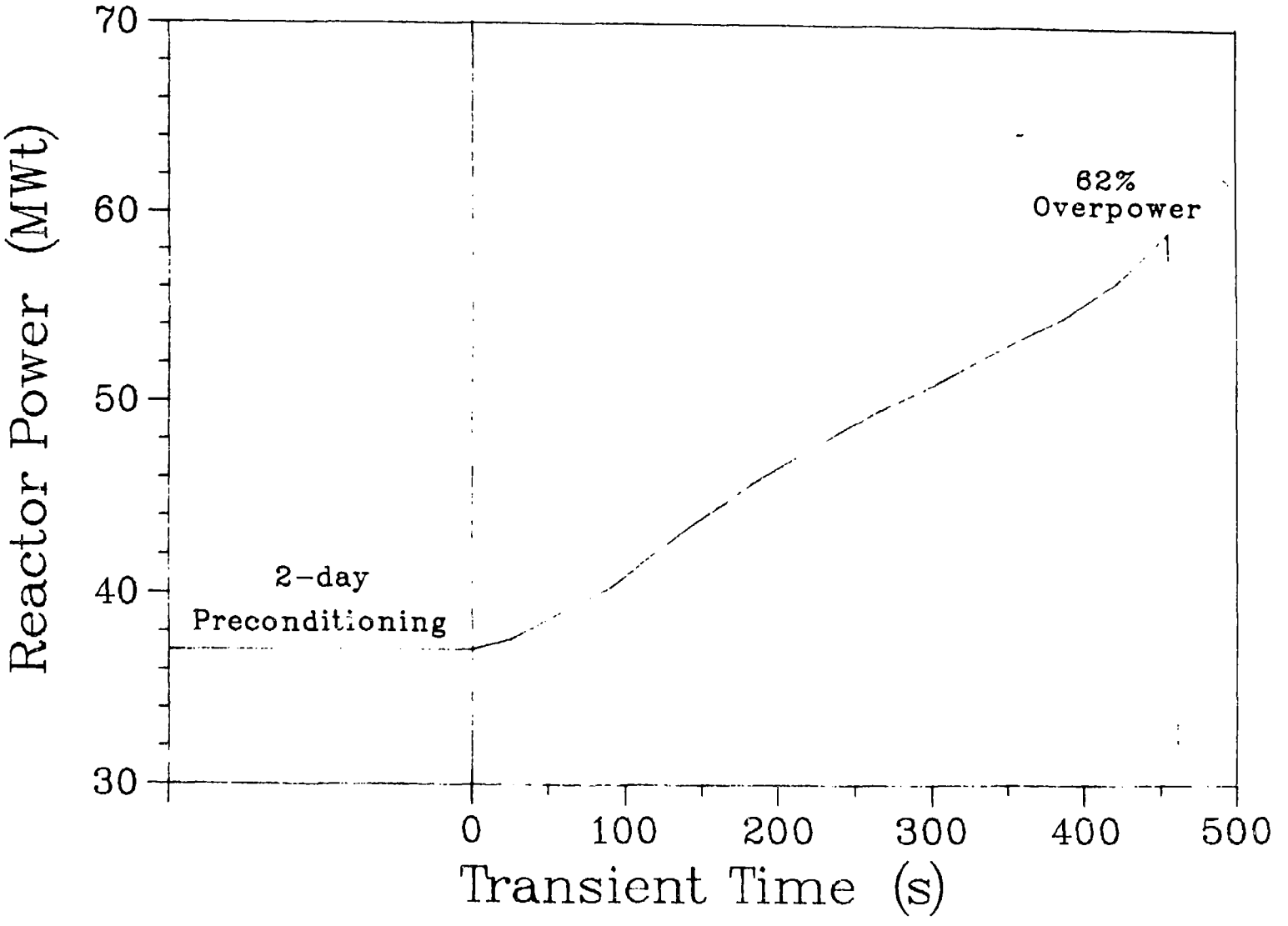

Fig. 1. EBR-II power history for the TOPI-1A test.

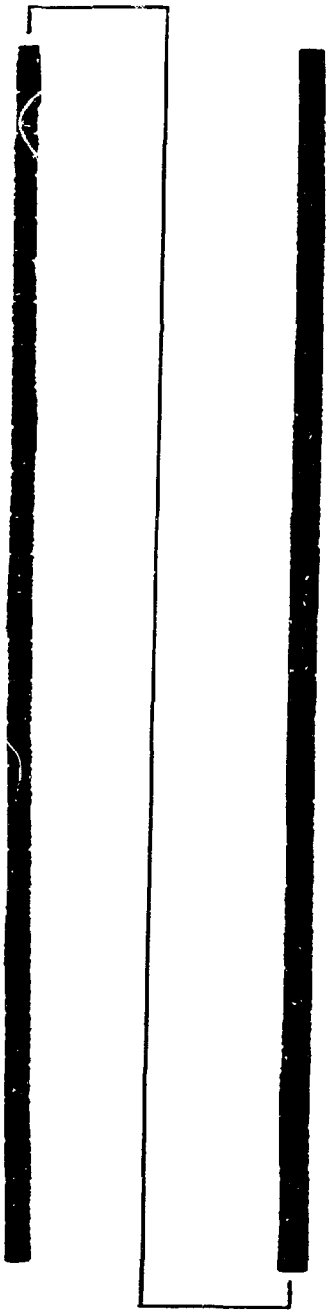

Fig. 2. Neutron radiograph of pin P40-C44 after the TOPI-1A test. Note uneven central void indicative of fuel melting.

Fig. 3. Neutron radiographs of pin P43-C29 before (left) and after (right) the TOPI-1A test. Area shown is between X/L = 0.54 and 1.00. Note agglomeration of solid fission products (dark) in the upper part of central void after the test.

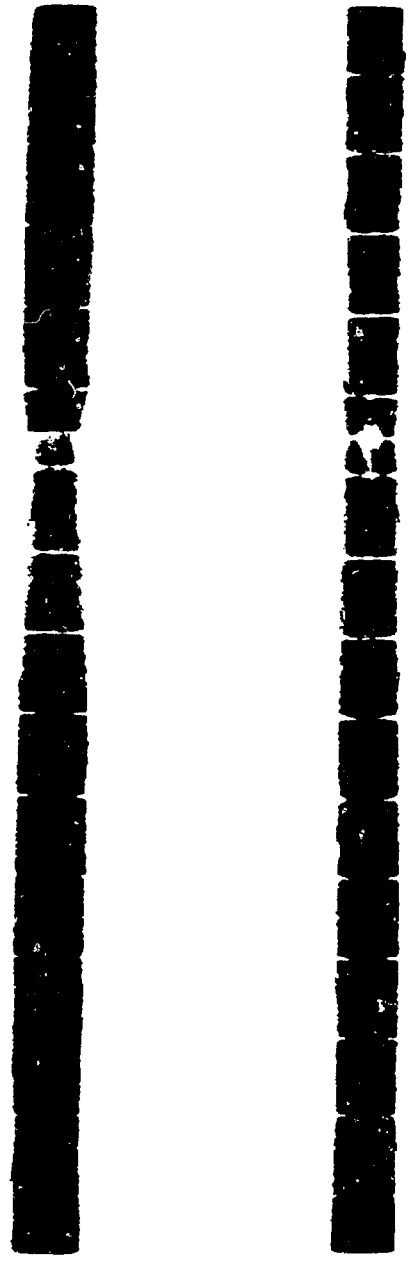

Fig. 4. Pre- (left) and post- (right) transient neutron radiographs of blanket pin W21-9 between X/L = 0.18 and 0.79. Filling of central void is evidence of fuel melting during transient. Note the precipitation of fission product ingots near the bottom.

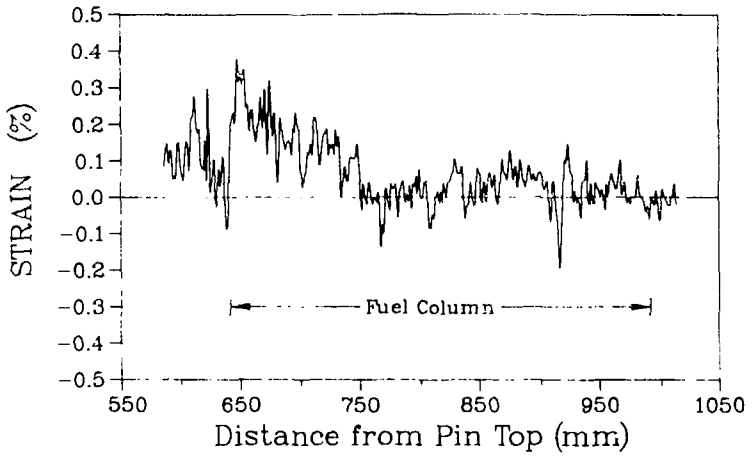

Fig. 5 Transient-induced cladding incremental strain in fuel pin P43-F104.

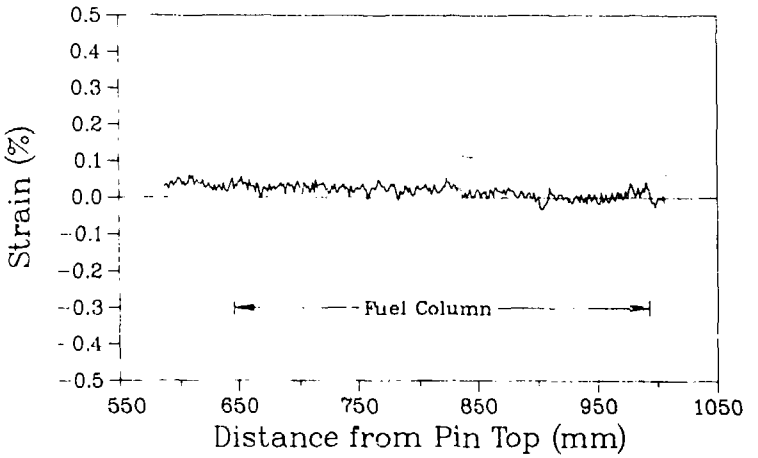

Fig. 6 Transient-induced cladding incremental strain in fuel pin P43-A5.

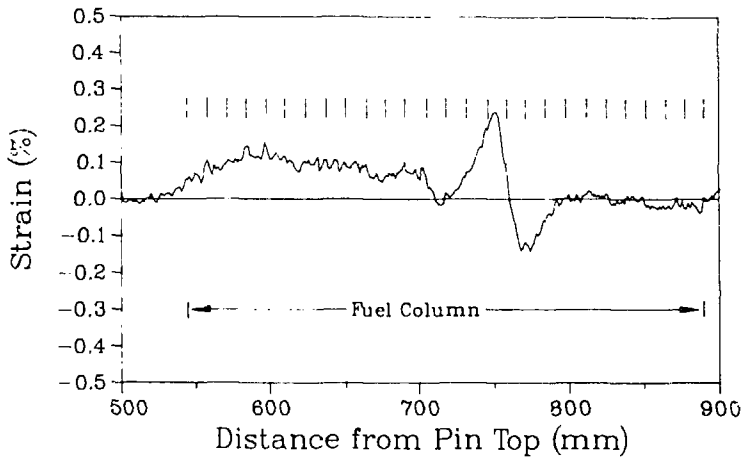

Fig. 7 Transient-induced cladding incremental strain in blanket pin W21-08.